



Voyager Observations of Galactic and Anomalous Cosmic Rays at the Termination Shock and in the Heliosheath

F.B. McDONALD¹

¹*Institute for Physical Science and Technology, University of Maryland, College Park, MD, USA*
fmcdonal@umd.edu

Abstract. On December 16, 2004 Voyager 1 crossed the heliospheric termination shock at 94 AU and began the exploration of the heliosheath. At the termination shock the observed intensity of anomalous cosmic rays > 4 MeV/n was much below that expected at what was generally believed to be their acceleration site while the galactic cosmic ray (GCR) intensity (150-380 MeV/n He) was close to its low solar maximum value. Based on the observations of Voyager 1 and Voyager 2 in the immediate foreshock region and of the initial 2.3 years of Voyager 1 in the heliosheath it is proposed that there were 3 major temporal effects that collectively produced the low anomalous cosmic ray intensity at the time of the termination shock crossing:

- a) The passage of the large interplanetary transients associated with the intense October/November 2003 solar events and subsequent solar activity played a major role in reducing the energetic particles over the ~ 4 month period prior to the termination shock crossing.
- b) The close correlation between the anomalous and galactic cosmic rays over cycle 23 suggests a long-term solar cycle modulation of the anomalous cosmic rays at the termination shock.
- c) There is a variation of the anomalous cosmic ray intensity associated with the reversal of the interplanetary magnetic field (IPB) at the termination shock over the cycle 23 solar maximum.

In 2007 the GCR He is approaching its expected solar minimum value at Voyager 1 and Voyager 2, and the effects of cosmic ray modulation in the heliosheath will soon be observable. In addition, there has been a significant increase in the intensity of 2.5 - 140 MeV electrons starting in the immediate foreshock region, providing the first direct observations of GCR electrons below 60 MeV. These electrons are especially sensitive to the passage of transients through the heliosheath.

Introduction

The complex interaction between the local interstellar medium (LISM) and the supersonic solar wind flowing out from the Sun defines our distant heliosphere, creating the heliosheath (Fig. 1) that plays an important role in the transport and acceleration of multiple energetic particle populations. In turn these energetic particles probe the properties and dynamics of the heliosheath and the termination shock at distances that extend beyond the Voyager Spacecraft.

As the ram pressure of the expanding solar wind approaches that of the local interstellar medium, there is a rapid transition through the for-

mation of a large, standing shock wave - the termination shock (TS). At this shock the radial velocity of the solar wind will decrease by a factor of $\sim 2.4 - 4$, depending on the shock strength. This velocity continues to decrease as $1/r^2$ (r is the heliocentric distance) out to the heliopause - the expected boundary layer between the decelerated solar wind and the LISM. The transverse component of the interplanetary magnetic field (IPB) jumps by the same shock strength factor and continues to increase $\propto r$ across the heliosheath. The heated and decelerated solar wind flows out around the termination shock and makes its way to interstellar space through the region of the heliotail that is produced by the motion of the solar system with respect to the local interstellar medium [1, 2, 3].

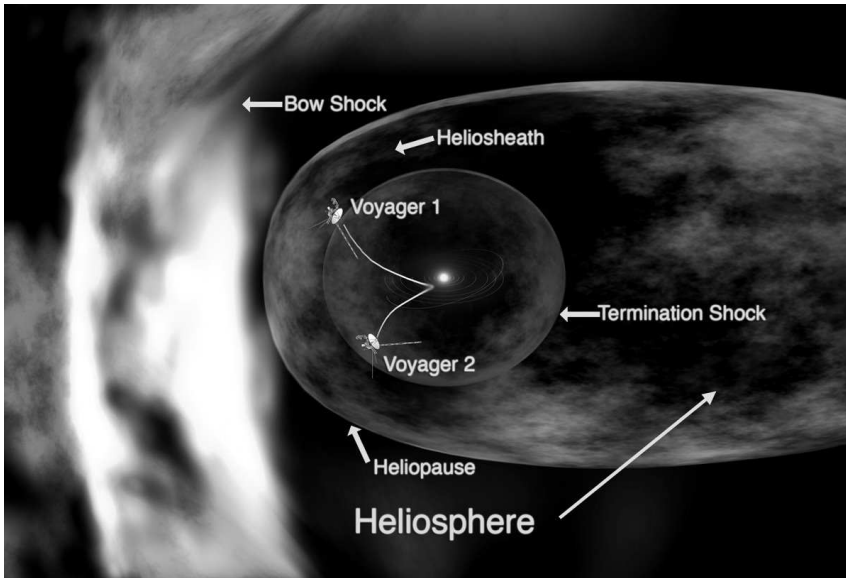


Fig. 1. The Heliosphere.

The heliosheath is the largest structure in our solar system. Its smallest dimension at the apex is estimated to be in the range $0.3 - 0.5 r_{ts}$ (where r_{ts} is the heliocentric distance to the TS) [4].

Galactic cosmic ray (GCR) ions and electrons entering the solar system must first cross the heliosheath and several studies have suggested they may experience significant modulation in this region [5, 6]. It is also possible there may be modest reacceleration of these GCRs as they traverse the TS [7, 8, 9]. The properties of GCRs below some 100 MeV should begin to emerge as Voyager 1 approaches the heliopause.

Anomalous cosmic rays (ACR) are predominantly singly-charge ions [10, 11, 12] that have their origin as interstellar neutrals, which have been ionized in IP space by charge-exchange or photoionization [13] and are convected out to the TS where it was assumed they would be accelerated to energies greater than some 50 MeV/n by the well-understood shock acceleration process [14]. The observed ACR charge composition is remarkably consistent with that expected from interstellar neutrals [15]. It had been expected that the ACR source spectra would be observed at the TS. Implicit in the ACR models was the assump-

tion that this source would not vary significantly with solar activity.

When V1 crossed the TS at 94 AU on December 16, 2004 [16, 17, 18], the 265 MeV/n GCR He was close to its 2001.25 solar maximum level, when radial gradient intensity corrections are applied. The 2.5 - 140 MeV electrons were at the detector background level and the ACR He intensities were a factor of 23 less than that expected for a weak shock (compression ratio $s = 2.40$) and a factor of 16 for a strong shock ($s = 4$) [15] and lower than had been observed by V1 over significant periods in the immediate foreshock region just after solar maximum.

In this highlight paper, the V1 ACR data from the inner heliosheath as well as that of V1 and V2 in the foreshock region are used to give an initial phenomenological interpretation of what is believed to be the principal processes producing this unexpected low ACR intensity level and to examine their evolution over the initial 2.3 year period following the TS crossing (TSX). The V1 GCR ions, as defined by 150 - 380 MeV/n He, exhibit a significant increase from its low state at the TSX toward the level expected for the solar minimum period of cycle 23. When compared to the V2 data,

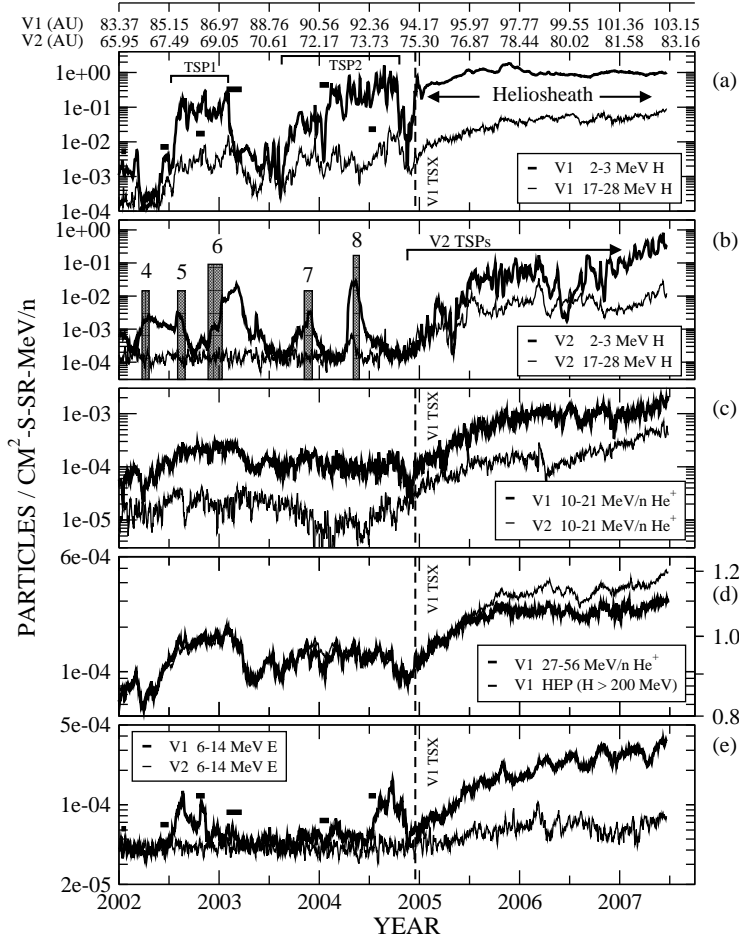


Fig. 2. Representative time histories of selected ACR and GCR components (5 day, moving average) from the Voyager CRS experiment [19]. The tall black rectangles (b) mark the passage of MIRs at V2 as defined by the increase in 2.5 MeV H and the decrease in GCR H > 200 MeV. The width of the MIR is determined from the onset of the decrease to the minimum value of the > 200 MeV H rate. The small black rectangles (a,e) are the estimated times these MIRs pass V1 using the V2 solar wind data to estimate the convection time from V2 to V1. The brackets in panels a and b mark the occurrence of termination shock particle events while the vertical dashed line is the time of the V1 termination shock crossing. The ACR and GCR intensities of panel d are each plotted on a different log scale that are then shifted to align the 2 data sets.

the effects of reacceleration at the TS appear to be small and the GCR intensity increase is dominated by changes in the modulation conditions inside the TS. Since crossing the TS there has been a strong continuing increase in the intensity of 2.5 - 140 MeV electrons starting in the immediate foreshock region with frequent decreases produced by the passage of transients through the heliosheath.

The Voyager CRS Experiment

The CRS Experiment on Voyagers 1 and 2 measures H intensity and spectra from 1.8 - 300 MeV; He 1.8 - 650 MeV/n; heavier nuclei to $Z=28$ and has the capability to resolve isotopes for $Z=1-14$ as well as for many isotopes in the $Z=15-28$ range, and 2.5 - 140 MeV electrons [19]. The experiment consists of 7 particle telescopes; 2 double-ended high energy telescopes, 4 low-energy telescopes and an electron telescope. After 30 years in space essentially the full capability of the experiment is still maintained although some of the redundancy has been lost.

ACRs, Termination Shock Particle Events, and Solar Interplanetary Particle Events

There are three major low-energy particle populations in the distant heliosphere:

(a) solar/interplanetary events (S/IP) that are convected out from the Sun by large transient merged-interaction regions (MIRs); (b) TSP events which generally persist for months in the foreshock region with episodes of streaming along the nominal direction of the interplanetary magnetic field [20, 21, 22] with a composition that resembles that of ACRs; (c) Anomalous cosmic rays. There is a strong interrelationship between these three groups. The MIRs that transport the S/IP events modulate the TSP increase and the ACRs. In addition, there is a strong interaction between the MIRs and the TS that produces large increases of electrons extending up to MeV energies and protons > 50 MeV.

An over view of each of these populations (Fig. 2) is provided by the time history of five different energetic particle populations in the foreshock region and the inner heliosheath from the

2002.0 post solar maximum period to 2007.4, approaching solar minimum. The V2 S/IP events are marked by rectangles (Fig. 2b) and the V1 and V2 TSP events by brackets (Fig. 2a,b).

(a) S/IP increases: Beginning with the Bastille day event (which arrived at V2 in 2000.9 at 62.9 AU [23, 24]), there was a series of 8 energetic particle increases that persist over some 3-4 solar rotations and occur at a quasi-periodic rate of ~ 150 days. These increases can generally be associated with specific periods of solar activity, are accompanied by increases in the solar wind velocity (V) and the IPB, and by moderate decreases in the galactic cosmic ray (GCR) intensity [18, 19, 20].

Of the 8 V2 S/IP increases (Fig. 3) 7 are associated with increases in V and IPB and with decreases in the > 70 MeV GCRs that allows the identification of events 5 and 7. Event 6 inversely mirrors the > 70 MeV rate but is different from the other 7 in that it is contained between 2 large MIRs as defined by the increases in V and the IPB [8]. The V1/V2 event 2 is well defined but there are no associated IP changes.

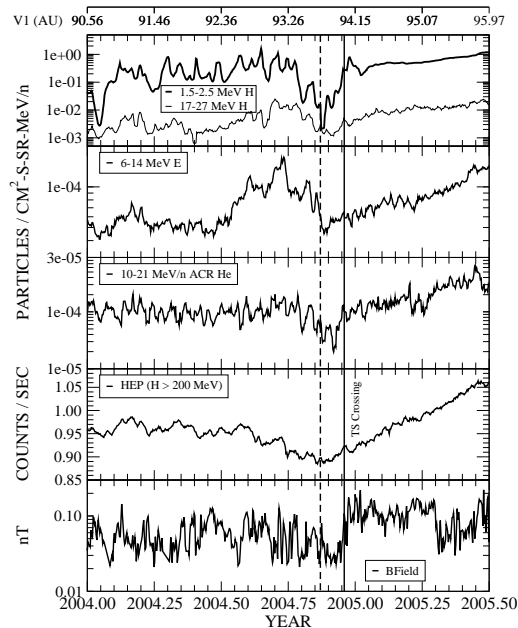


Fig. 3. V1 time histories of selected ACR and GCRs (5 day moving average) and the magnetic field data [16] (1 day average) from 2004.0 - 2005.5. The dashed line marks the trailing edge of the MIR and the solid line is the TSX.

Because of the higher rigidity of the GCRs, the > 70 MeV integral rate decreases (Fig. 2d) reflect the properties of the IP disturbances over a greater volume of space that extends beyond the spacecraft. The onset of the GCR decreases and the time of minimum intensity are taken as a measure of the width of the MIRs that are controlling the low-energy S/IP ions. These MIR boundaries are shown as shaded rectangles in figures 2a,e.

Despite the V1 and V2 separation of 90 AU and 60° in heliolatitudes, there is a reasonable correspondence between their time histories for the first 4 S/IP events after a convection correction of 0.19 years has been applied using the solar wind speed measured at V2. This correspondence establishes the extended nature of these S/IP events.

(b) Termination Shock Particle Events:

In mid-2002, some two years after the cycle 23 solar maximum, there began an unusual increase of MeV ions and electrons at Voyager 1 (85 AU) [20, 21] that persisted for some 6 months at intensity levels at least 20 times and sometimes 500 times greater than that at Voyager 2 (68 AU) (Figs. 2, 3). In 2003.7 there was a second year-long increase that reached even higher intensity levels. Over this period these unusual enhancements are durable features of the distant heliosphere and must be related to the close proximity of Voyager 1 to the TS. These TSP events are characterized by temporal variations on a variety of time scales, frequent periods of streaming along the expected direction of the interplanetary magnetic field, relatively flat energy spectra and a charge composition at low energies resembling that of anomalous cosmic rays as defined by the high O/C ratio [20, 21, 22].

TSP and S/IP-MIR interactions: The IP transients (Fig. 3) play a major role in producing the large scale variability observed in the two V1 TSP events. TSP 1 and 2 start immediately after the predicted passage of MIRs associated with events 4 and 7. Event 6, with its flanking IPB and V peaks, is associated with the termination of TSP 1. The MIR of event 7 produces a rapid decrease in the 2.5 MeV ion intensity of TSP 2, briefly reducing it to the level of the V2 S/IP event. Event 8 at V2 is the product of the Halloween series of large solar events that had occurred in the Sun's southern hemisphere some 6 months earlier, resulting in

the largest cycle 23 S/IP ion increase yet observed at V2.

At V1 in the northern hemisphere the effect on GCRs and ACRs is greater than that observed for the previous events. The GCR decrease (Figs. 2, 3) takes place over a period of 3 months through a series of step decreases with 265 MeV/n He being reduced to its 2002.25 solar maximum level (when a radial gradient correction is applied) and the 10 - 21 MeV/n ACR He is at the lowest level in cycle 23. There are large increases of 2.5 - 20 MeV electrons and $H > 40$ MeV associated with this MIR. The magnetometer experiment shows an unusually disturbed period with multiple increases of the IP magnetic field extending above 0.12 nT [16].

On 2004.87, some 33 days before the TS the IPB decreased below 0.024 nT and the ACRs and GCRs began to increase. At the TS there was a sharp increase in the magnetic field and in lower energy ions $< \sim 4$ MeV [16, 17, 18]. However, the TSX had no effect on GCR ions and electrons but there was a small peak in the ACR intensity > 4 MeV/n. These ACR and GCR intensities continued to increase in the heliosheath at an exponential rate for almost a year after the 2004.87 minimum level.

At V2 the onset of the TSP increase begins near 2004.87 and has continued through mid-2007. The intensity level and variability of 2.5 MeV H are very similar to that observed for the V1 TSP increases (Fig. 2).

A comparison between the V1 GCR and ACR intensity changes in the heliosheath and those of V2 in the foreshock region 1 from 2004.92 - 2007.0 shows a close correspondence between the two data sets (Fig. 4) (*i.e.* TSPs are a good monitor of ACRs in the inner heliosheath). It also establishes that the changes in the ACR and GCR intensities are predominantly temporal and not spatial. What is being observed at this particular time is a recovery from the strong transients in late 2004 along with the changes in modulation conditions in the recovery toward the cycle 23 solar minimum period.

There is a strong correlation in the V1 data between changes in the integral GCR rate > 200 MeV and 30 - 56 MeV/n ACR He that extends from the onset of TSP 1 in 2002.54 through 2007.35 (Fig. 2). This relation of the relative

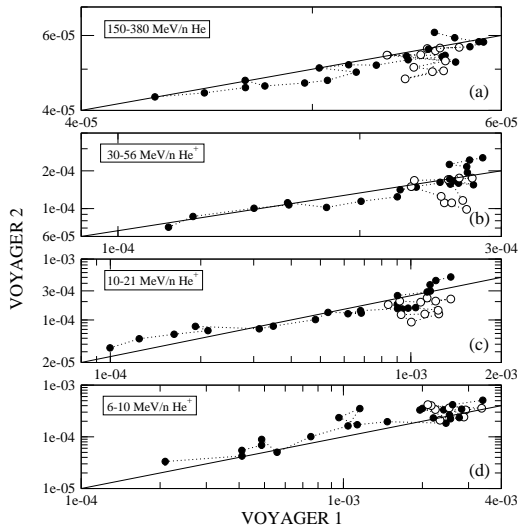


Fig. 4. Plot of V1 vs. V2 ACR and GCR intensities (26 day average) from 2004.92 at the V1 TSX and the onset of the V2 termination shock particle event to 2007.35. The open circles mark the passage of a large transient at V2. The effect of this transient is to reduce the intensities of GCRs and ACR He > 10 MeV/n and to accelerate lower energy ACRs. The solid line in each panel is of slope one.

changes in the GCRs and ACRs is examined in greater detail using cross-correlation plots over the period 2001.64 - 2007.25 of 265 MeV/n GCR He versus 3 energy intervals of ACR He extending from 6 - 56 MeV/n (Fig 5). Also shown are cross-correlation plots between these ACR He groups. In the fore-shock region the ACRs and GCRs are recovering along the straight regression line. The effect of MIRs is to move the ACRs and GCRs back down this regression line. After the TSX this regression line changes slope with the change being larger for 10 - 21 MeV/n ACR He than for 6 - 10 MeV/n and 30 - 56 MeV/n ACR He (Fig. 4). Based on the similarity of the V2 TSP and the V1 heliosheath increase this change is predominantly temporal and not spatial and reflects the recovery toward solar minimum conditions. For a major part of solar cycle 23 there is a close relation between the ACR intensity near the TS and that of GCR (Fig. 4).

(c) ACRs and the 22 Year Heliomagnetic Cycle:

It is useful to examine V1 and V2 regression plots of the intensity of 15.5 MeV/n He versus 43 MeV/n He (Fig. 6). For V1 there is a straight line fit from 1997.0 to 2001.35 followed by a 95 ± 12 day transition to a new regression line. The V2 ACR He⁺ follows a similar pattern except the transition occurs a month later over a 128 day period. However a regression plot of the intensity of higher rigidity GCRs (300 - 450 MeV/n He) versus 30 - 56 MeV ACR He (Fig. 6c) gives a straight line fit from 1997.0 - 2006.1.

These ACR spectral transitions are interpreted as marking the time of the reversal of the heliospheric magnetic field at the TS. These reversal times can be traced back to the Sun using the V2 solar wind velocities and a deceleration correction for the effect of pick-up ions derived by Wang and Richardson [25] along with the estimates of the location of the TS, which were normalized to the V1 TS crossing [26]. This procedure gives a time of the onset of reversal in the northern IPB field near the Sun starting in early June 2000 and a completion time of early August 2000. The transition time at the Sun in the southern hemisphere extends from mid-June to early October, 2000.

Wang, Sheeley and Andrews [27] used a potential field source surface analysis (2.5 AU) of a photospheric magnetic field map to determine the times of the polarity reversal near the Sun: North, Jan- April, 2000; South, June-November, 2000. The Voyager results are in reasonable agreement with those of Wang *et. al.* [27].

Observations of the reversal of the photospheric magnetic field are found to occur much later (~ 15 months on the average) [28, 29, 30, 31] than the reversal observed for the IPB field.

Wang *et. al.* [27] found that most of the IP open field lines originate in active region latitudes from small coronal holes with strong footprint fields and a predominately slow solar wind. In this model the IPB field reflects what is happening at latitudes below the polar regions. The changes in the ACR intensity producing the transitions seen in figure 5 are modest. At V1 it is due to the increasing intensity of 30 - 56 MeV/n ACR He while at V2 the transition time is controlled by the decrease of ACR He below ~ 20 MeV/n [Fig. 7] [32].

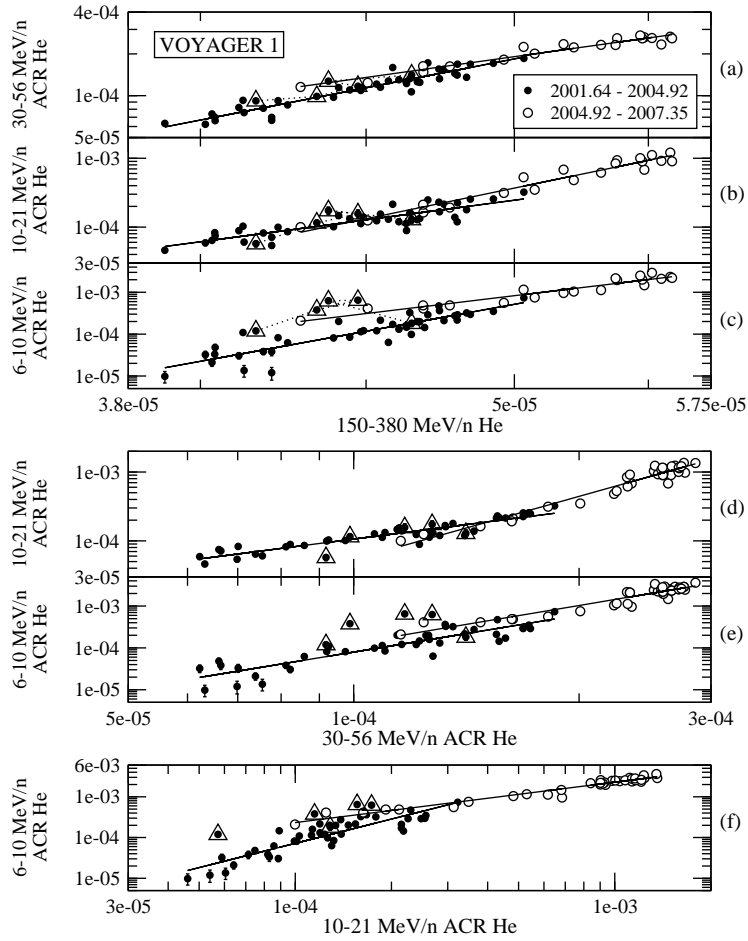


Fig. 5. Regression plots (26 day averages) of GCR He vs ACR He and various combinations of ACR He. The solid line is a least squares fit for the 2 time periods, one before the TSX and 2004.92 - 2007.35 when V1 is in the heliosheath. The triangle points are associated with the passage of a transient and have not been used in the analysis. The contribution of ACR He to the GCR 150 - 380 MeV/n He is $< 3.5\%$ and no correction has been applied.

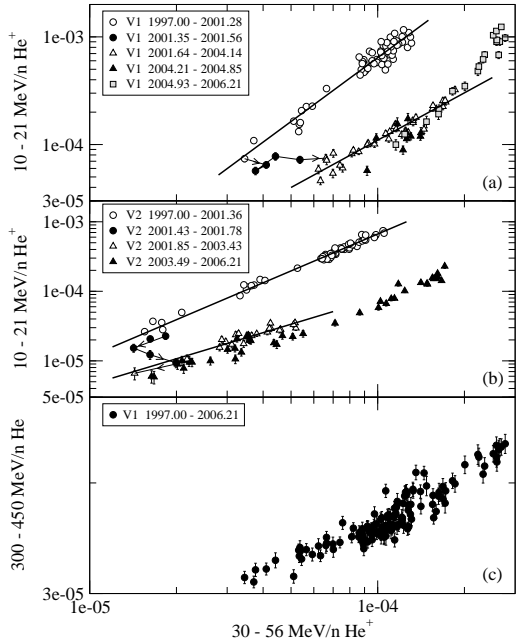


Fig. 6. Regression plot of 10 - 21 MeV/n He⁺ (V1, V2) and 300 - 450 MeV/n GCR He (V1) vs 30 - 56 MeV/n He⁺ for the periods shown in Figure X. The top solid lines are least squares fits to the data from solar minimum to solar maximum. After the transition a shorter time interval is selected. The data times shown are the beginning of each 26 day interval.

Discussion

The close association between ACR intensities in the inner heliosheath and those of the V2 TSP events establishes that these changes are mainly temporal and not spatial and makes possible the extension of the inner heliosheath ACR observations back to the onset of the 1st V1 TSP event in 2002.54. There is a well-defined long-term variation of the ACRs at TS mid-latitudes over this 5-year period that is associated with the passage of large IP transients. The correlation between the ACR and GCR intensities over this ~ 0.5 solar cycle suggest that both components exhibit a solar cycle variation that reflects the role of changing solar activity but which may involve different physical processes for the two components. In addition there is the 22-year variation associated with the reversal of the IP magnetic field.

The regression plots of figure 5 provide insight into the nature of the processes involved in the long term variation. The 6 panels in this figure show straight line fits of slope D from the time of the completion of the reversal of the IPB field in the northern hemisphere: 2001.69 to \sim 2004.9. Around this time there is a distinct change in the slope of the regression lines, D, that persists through 2007.35. For a given straight-line interval for the period t_1 to t_2 :

$$\begin{aligned} D &= \frac{\log J_{He^+}(t_1) - \log J_{He^+}(t_2)}{\log J_{GCR}(t_1) - \log J_{GCR}(t_2)} \\ &= \ln \frac{J_{He^+}(t_2)}{J_{He^+}(t_1)} / \frac{J_{GCR}(t_2)}{J_{GCR}(t_1)} \end{aligned}$$

There is a well-defined pattern in the data. The slope of the 10 - 21 MeV/n He⁺ versus GCR He (Fig. 5b) and versus 30 - 56 MeV/n He⁺ (Fig. 5d) become steeper after 2004.9 while 6 - 10 MeV/n He⁺ versus 30 - 56 MeV/n He⁺ (Fig. 5e) does not change significantly over the 5.5 year period.

Such a pattern was predicted by Florinski and Zank [33] in a model examining the interaction of an MIR with the TS. The MIR crossing the TS produces a forward shock / reverse shock pair followed by a forward / rarefaction pair. This interaction changes the location and compression ratio of the TS. The effect on the ACRs is to produce a “bowed” energy response with a much larger depletion of intermediate energy ACRs than that of higher and lower energy ACRs, which is what is observed in the V1 data. Florinski and Zank attribute the reduced response at higher energies to the larger diffusive mean free paths of the higher rigidity ACRs while at lower rigidities the acceleration time is much shorter. This result is consistent with the detailed study by Cummings *et al.* [34] of the ACR spectra from the CRS experiment that establishes the ACR spectra are evolving toward the expected form through the preferential enhancement of intermediate-energy ACRs.

However the V1,V2 ACR He spectra in mid-2007 (Fig. 7) indicates other factors may be involved. At this time V2 is very close to the TS while V1 has moved deeper into the heliosheath. Despite the fact that the rate of increase of ACR He is the same at both spacecraft (Fig. 2), there remain large differences in their intensity in the 10 - 25 MeV/n He intermediate energy range. At this time

the V1 spectra show the expected power-law spectra at lower energies with an exponential roll-off at energies > 25 MeV/n. At V2 there is a power-law spectrum at low energies but from 10 - 30 MeV it is essentially flat at a level some 4 times smaller than that of V1. Above 30 MeV/n there is an exponential roll-over with an intensity level close to that of V1. While V2 is assumed to be sampling the mid-latitude region of the TS, V1 must either have some connection to an additional source or there is a N-S asymmetry in the source region.

Schardron and McComas [35] have previously examined the strongly correlated modulation of V1 ACRs and GCRs from the CRS experiment for the same periods reported here using both a 1D diffusion convection model and a 1D time dependent modulation equation. They find reasonable agreement when the ACR and GCR source are close together and at a location well beyond V1, *i.e.* both ACRs and GCR follow approximately the same modulation path. They favor placing the ACR acceleration site at the flanks of the heliosheath but do not rule out sources deeper in the heliosheath. It may also be possible that the polar regions may be involved or there is a N-S asymmetry.

Cosmic Ray Modulation in the Distant Heliosphere

Observations from the heliospheric network (Pioneer 10 through 1996, V1, V2, Ulysses, IMP 8 and ACE) beyond 1 AU now span more than 1.6 heliomagnetic cycles and extend across the TS into the heliosheath. In this section the focus is on the GCR data from cycle 23 through 2007.5 and on comparisons of this period with the solar minimum and maximum intensities from previous cycles back to the 1977 solar minimum period. The GCR He (265 MeV/n) data for cycle 23 are shown in figure 8 (26 day averages) for the period 1997.0 - 2007.5. At 1 AU the solar minimum (1997) and solar maximum (2000.6) intensity is very close to those of cycle 21, with decreases by a factor of 4.5 for each cycle. However, at V2 (63.5 AU) the reduction was 33% and 22% at V1 (81 AU). Essentially all of the modulation associated with this 11-year solar cycle occurs in the region of the supersonic solar wind.

After solar maximum there was a small recovery in late 2000 at 1 AU followed by a ~ 2.5 year

plateau period, which is different from previous recoveries in the neutron monitor era. Significant recovery began immediately following the intense solar activity in late 2003 and by mid-2007 the 1 AU intensity is very close to that of the 1997 cycle 22 solar minimum. This pattern is essentially repeated at V2 but with a 6 month convection delay. At V1 the minimum intensity at solar maximum occurs at the expected time but there are significant increases relative to V2 associated with TSP 1 and 2. These increases produce large increases in the GCR and ACR radial intensity gradients [36]. After the TSX crossing the V1 and V2 intensities are very close over the 2.5 year period except for the passage of a large transient at V2 in March 2006.

As they travel outward the Voyagers and Pioneer 10 (when it was available) sample a different region of space over each phase of the solar and heliomagnetic cycles. To obtain a more complete description of the spatial variations it is useful to combine the data from multiple cycles. One method is to focus on the solar minimum and solar maximum period from successive cycles and to normalize the data using the 1 AU intensities (Fig. 9). In fact the 1 AU solar minima and solar maximum intensity of cycle 23 is very close to that of cycle 21. The normalization correction is only significant for the cycle 22 solar maximum. For all 3 cycles the solar minimum radial intensity gradients, g_r , are not very different between 1 and 10 AU. For the combined cycle 20 and 22, g_r is essentially zero between 15 and 70 AU. Cycles 21 (1987) and 23 (2007) solar minima occur in $q_A < 0$ epochs when GCR ions enter along the heliospheric neutral current sheet and exit over the polar regions. For these solar minimum periods the GCR radial distribution is steeper, and a radial gradient of 20%/AU is maintained out to the vicinity of the TS. The GCR He data from 4 solar minimum and 3 solar maximum periods show a strong ordering of the data over an extended spatial range near the ecliptic plane.

Discussion

(a) The radial intensity gradient, g_r are different, especially beyond 15 AU for $q_A > 0$ and $q_A < 0$ solar minima.

(b) The change in g_r are significantly smaller in the inner heliosphere (< 15 AU) consistent with

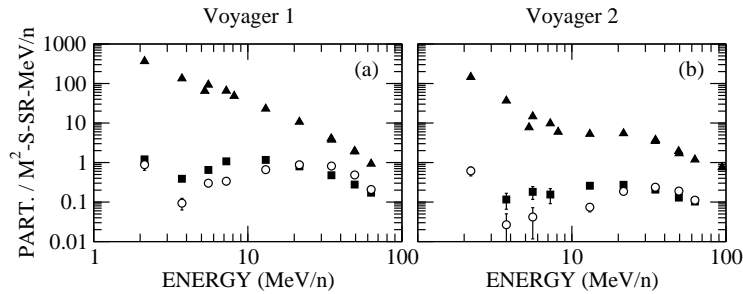


Fig. 7. V1, V2 combined ACR and TSP He^+ spectra for time periods just prior to the transition time [Filled Square: V1 03/20 - 04/15/2001 (80.7 AU), V2 04/15 - 05/11/2001 (63.9 AU)] and just after the transition time [Open Circle: V1 08/23 - 09/18/2001 (82.2 AU), V2 12/05 - 12/31/2001 (65.8 AU)]. The solid triangles are from 06/04 - 07/27/2007 for both V1 and V2.

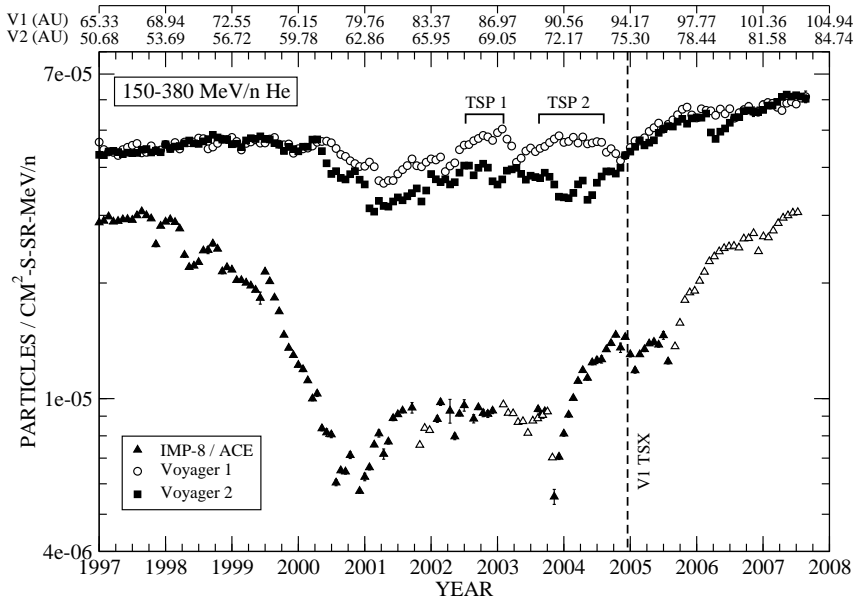


Fig. 8. Cycle 23 time history of 265 MeV/n GCR He (26 day average) at 1 AU and from V1 and V2.

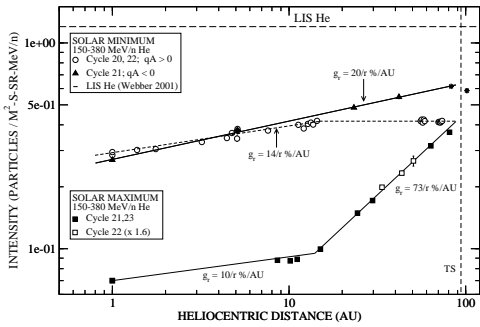


Fig. 9. Intensity of 265 MeV/n GCR He at solar minimum and solar maximum from 1977 to 2007 using data from IMP8, Pioneer 10 and Voyagers 1 and 2. The cycle 22 solar maximum data has been normalized using the 1.6 ratio of the cycles 21 and 23 solar maximum intensity at 1 AU to that of cycle 22.

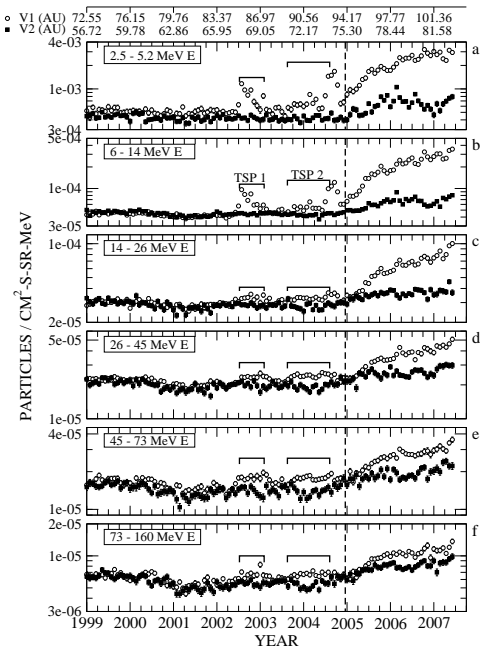


Fig. 10. Time histories of the 6 V1, V2 electron channels (26 day averages) from 1999 to 2007.5. The V1 TSP events are marked by brackets and the time of the TS crossing is shown as a vertical dashed line. The first V2 TSP event begins just before the V1 TSX.

the small changes observed at 3 AU using the IMP 8/Ulysses data [37].

(c) The extrapolation of the cycle 20 and 22 solar minimum data to that of solar maximum intersect at 89 AU, close to the actual TSX, suggesting there was not a significant change in the he-

liosheath modulation from 1997 to 2001.3. This is consistent with the small decrease (22%) in the V1 GCR intensity. There is a marked change near 15 AU in g_r at solar maximum - *i.e.* the major changes producing the 11 year modulation cycle occur between ~ 15 AU and the TS.

(d) Based on the latest estimate of the local interstellar energy spectra [38] and a heliosheath thickness of 40 AU an average value of $g_r \sim 1.7\%/AU$ is expected in the heliosheath. From 2005 - 2007.5, $g_r = 1.04 \pm 0.2$ if all the increase is spatial and not temporal. This value of g_r may increase as V1 travels deeper into the heliosheath.

(e) At V1 in the heliosheath the GCR He intensity is some 3% lower than at V2. This difference may reflect a very small reacceleration effect at the TS [7]. It could also be due to asymmetries between the N and S hemispheres due to the orientation of the local interstellar B field as predicted by Opher *et. al.* [39].

Galactic Cosmic Ray Electrons

At energies below some 100 MeV, GCR electrons are the source of the lower energy diffuse gamma and x-ray emission from the galaxy and may play a major role in ionizing and heating the interstellar medium. These lower energy electrons are produced as knock-on electrons as well as directly accelerated primaries and interstellar secondaries from the decay of charged pions. Within the heliosphere these electrons are strongly modulated even at solar minimum. In the inner heliosphere the dominant electron component below ~ 60 MeV are of Jovian origin.

The Voyager CRS experiment [19] has two telescope systems that respond to electrons: the High Energy Telescope (HET), 2.5 - 10 MeV E, and the Electron Telescope, 6 - 160 MeV E [19] (Fig. 10). Except for periods when there are large fluxes of electrons of Jovian or solar origin, the response of these telescopes have been dominated by background produced by high energy protons. For example, over the 1987 solar minimum at 22 AU all electron channels exhibit a negative latitudinal gradient similar to that obtained for GCR and ACR ions instead of the positive latitudinal gradients expected for electrons in a $qA < 0$ epoch.

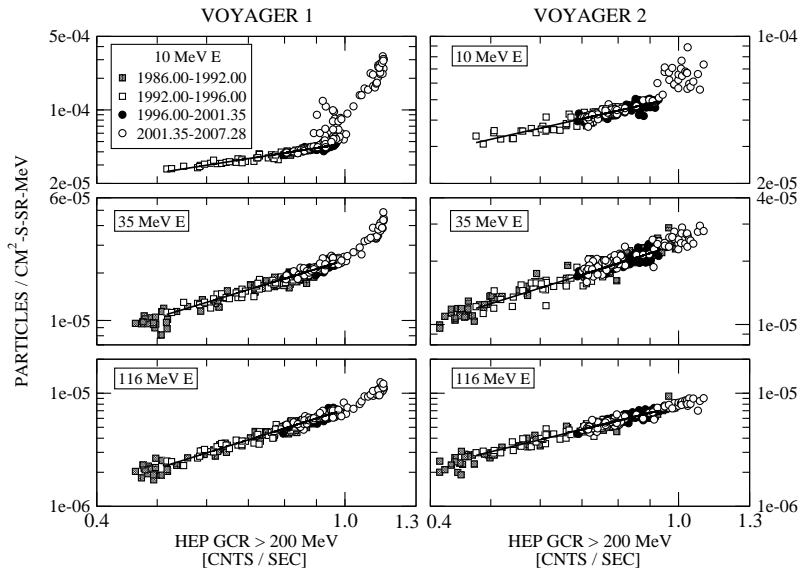


Fig. 11. Cross-correlation of selected V1 and V2 electron channels vs the HEP (GCR $H > 200$ MeV) rate from 1986 to 2007.28. This rate also responds to electron > 10 MeV but their contribution at this time is $< 1\%$. The background in the electron channels is mainly produced by high energy protons. Prior to 2004.4, the electron rates are dominated by background.

However, at the beginning of the first V1 TSP event there was an increase in the 2.5 - 70 MeV electron intensity at V1 with no corresponding increase at V2. There are large increases in the 2 - 20 electron intensity over the next 2.4 years associated with the passage of transients through the interstellar medium. At 2004.87 just after the passage of the large compound transient and just prior to the TSX all of the V1 electrons are at background level. The electron time histories in the V2 TSP event that starts at this time and extends through 2007.5 are very similar to the V1 TSPs 1 and 2.

The V1 electrons immediately after the pre-TS minimum increase at an exponential rate for ~ 0.45 years and then at a slower rate over the next several years.

At the higher electron energies (> 26 MeV) the background levels are still significant at V1. This background is produced by higher energy GCR H. A plot of HEP GCR (integral rate of $H > 200$ MeV) (Fig. 11) for representative V1, V2 electron energy channels for the period 1986 - 2007.3 show the high background still present in the 116 MeV E channel and the absence of any increases at V2 above 26 MeV.

The V1 background-corrected electron time histories (Fig. 12) all show a continuing increase in intensity as V1 moves to greater heliocentric distances in the heliosheath. There are probably 2 major processes involved: the continuing return to solar minimum conditions and a positive g_r in the heliosheath. The rate of increase after 2005.45 gives an upper limit of $g_r = \sim 18\%$ in the 5 channels above 6 MeV in the inner heliosheath.

The V1 energy spectra (Fig. 13) (1/26 - 3/19/07, 101.86 AU) has a spectral slope of $\gamma = 1.5$. Webber *et al.* [40] using data on the low-frequency galactic non-thermal ratio emission and Strong *et al.* [41] using low-energy galactic continuum gamma-ray emission have obtained estimates of the interstellar electron spectra. However, Strong *et al.* [42] and Langer [43] show that plausible changes in the interstellar parameters can produce large changes in the calculated LIS spectra. The spectrum shown in figure 13 is Langer's estimate of the most probable LIS electron spectra. Over the energy range 10 - 100 MeV it has a spectral slope $\gamma = 1.66$.

The V1 electron intensities should continue to increase toward interstellar intensities as V1 approaches the heliopause. These low-energy elec-

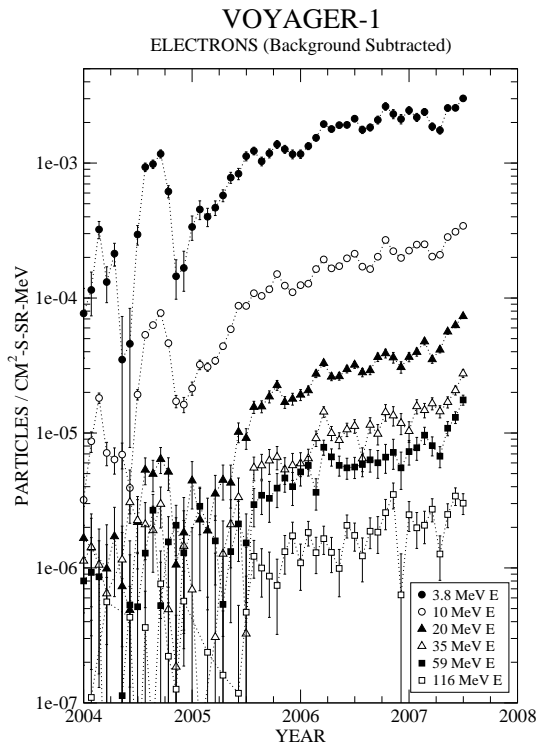


Fig. 12. Time history (26 day average) of V1 electrons with the background subtracted for the 2004 to 2007.5 time period. The continuing increase after ~ 2005.5 is assumed to be a superposition of spatial and temporal effects.

trons should provide a very sensitive measure of changes in modulation conditions associated with the onset of cycle 24 in the near future.

The Future

The large TSP event in progress at V2 suggests that it will cross the TS in the near future. This encounter should occur under relatively quiet conditions and provide an opportunity to observe the ACRs at the TS near solar minimum conditions. As solar activity increases in cycle 24 it would be expected that the ACR intensity would decrease as was the case for cycle 23 (Figs. 3 and 4) and at some point the ACRs will also decrease as the Voyagers approach the heliopause. For galactic cosmic rays, it will be possible to begin studying ions at energies < 100 MeV/n, to estimate their energy density, to study their effect of the energy loss by

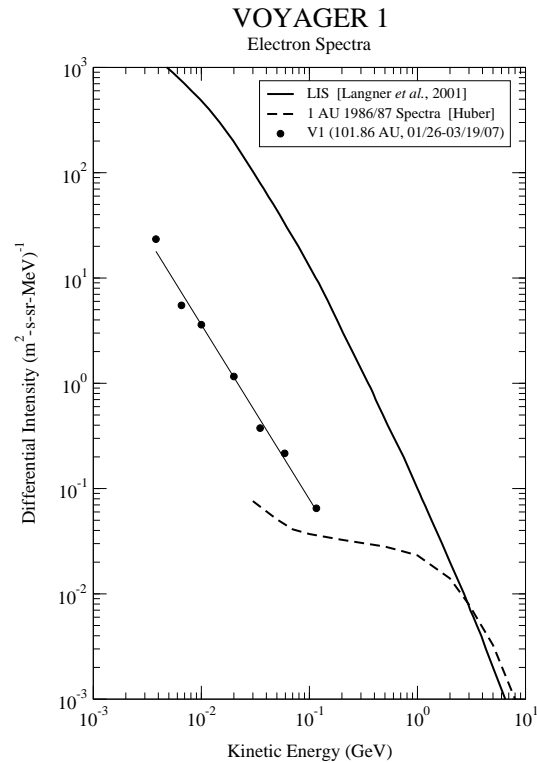


Fig. 13. V1 electron energy spectra at 101.86 AU. Shown for comparison is the interstellar spectra adopted by Langer [43] and the 1 AU 1986/87 spectra of Huber [44].

ionization in interstellar space on different charge species and perhaps even encounter new low energy particle populations. The GCR electrons will be especially sensitive to changes in modulation conditions in the heliosheath while still increasing at a rapid rate toward their local interstellar values. Based on the 35 years of exploration beyond 1 AU, it has also become the norm to expect the unexpected.

References

- [1] T.E. Holzer, *Ann Rev Astron. and Astrophysics*, 27 (1989) 199.
- [2] S.T. Suess, *Rev Geophysics*, 28 (1990) 97.
- [3] G.P. Zank, *Sp. Sci. Rev.*, 89 (1999) 413.
- [4] D.A. Gurnett, *Geophys Res. Lett.* 30 (2003) 2209.
- [5] F.B. McDonald et. al, *J. Geophys Res.* 107 (2002) 1029.

- [6] W.R. Webber and J.A. Lockwood, *J. of Geophys Res.* 106 (2001) 29333.
- [7] J.R. Jokipii, J. Kota, and E. Merenyi, *J. Astrophys.* 405 (1993) 782.
- [8] C.D. Steenberg. Ph.D. Thesis, Potchefstroom University, South Africa, 1998.
- [9] M.S. Potgieter and S.E.S. Ferreira, *J. of Geophys Res.* 107 (2002) 1089.
- [10] J.H. Adams et. al., *Astrophys J.* 375 (1991) L45.
- [11] B. Klecker et. al., *Astrophys J.* 442 (1995) L69.
- [12] R.A. Mewaldt et. al., *Astrophys J.* 446 (1996) L43.
- [13] L.A. Fisk, B. Kozlovsky, and R. Ramaty, *Astrophys J.* 190 (1974) L35.
- [14] M.E. Pesses, J.R. Jokipii, and D. Eichler, *Astrophys J.* 246 (1981) L85.
- [15] A.C. Cummings, E.C. Stone, and C.D. Steenberg, *Astrophys J.* 578 (2002) 194.
- [16] L.F. Burlaga et. al., *Science* 309 (2005) 2027.
- [17] R.B. Decker et. al., *Science* 309 (2005) 2020.
- [18] E.C. Stone et. al., *Science* 309 (2005) 2017.
- [19] E.C. Stone et. al., *Space Sci. Rev.* 21 (1977) 355.
- [20] F.B. McDonald et. al., *Nature* 426 (2003) 47.
- [21] S.N. Krimigis et. al., *Nature* 426 (2003) 45.
- [22] A.C. Cummings et. al., *AIP Conf. Proc.*, 2006, Vol. 858, p. 86.
- [23] L.F. Burlaga et. al., *Solar Physics* 204 (2001) 399.
- [24] C. Wang, J.D. Richardson, and R.P. Lepping, *Solar Physics* 204 (2001) 411.
- [25] C. Wang and J.D. Richardson, *J. Geophys Res.* 108 (2003) 1058.
- [26] J.D. Richardson, C. Wang, and M. Zhang, *AIP Conf. Proc.*, 2006, Vol. 858, p. 110.
- [27] Y.M. Wang, N.R. Sheeley Jr., and M.D. Andrews, *J. Geophys Res.* 107 (2002) 1465.
- [28] I.A. Bilenko, *Astron Astrophys.* 396 (2002) 657.
- [29] C.J. Durrant and P.R. Wilson, *Solar Physics* 214 (2003) 23.
- [30] N. Gupalswamy et. al., *Astrophys J.* 598 (2003) L63.
- [31] K.L. Harvey and F. Recely, *Solar Physics* 211 (2002) 31.
- [32] F.B. McDonald et. al., *Geophys Res. Lett.* 34 (2007) L05105.
- [33] V. Florinski and G.P. Zank, *Geophys Res. Lett.* 33 (2006) L15110.
- [34] A.C. Cummings et. al., *Proceedings of 30th ICRC, Merida, 2007, Vol. 6, p. 255.*
- [35] N.A. Schwadron and D.J. McComas, *Geophys Res. Lett.* 34 (2006) L14105.
- [36] F.B. McDonald et. al., *Proceedings of 29th ICRC, Pune, 2005, Vol. 1, p. 34.*
- [37] F.B. McDonald et. al., *Adv. Space Res.* 23 (1999) 453.
- [38] W.R. Webber and J.A. Lockwood, *J. Geophys Res.* 107 (2001) 323.
- [39] N. Opher, E.C. Stone, and P.C. Liewer, *Astrophys J.* 640 (2006) L71.
- [40] W.R. Webber, G.A. Simpson, and H.V. Cane, *Astrophys J.* 236 (1980) 448.
- [41] A.W. Strong et. al., *Astron Astrophys.* 292 (1994) 82.
- [42] A.W. Strong, I.V. Moskalenko, and O. Reimer, *Astrophys J.* 236 (1980) 448.
- [43] V.W. Langer, O.C. de Jager, and M.S. Potgieter, *Adv. Space Res.* 27 (2001) 517.
- [44] D.M. Huber, Ph.D. Thesis, University of Delaware, 1998.